Classifying Anti-Nuclear Antibodies HEp-2 Images: A Benchmarking Platform

Peter Hobson[*], Brian C. Lovell[†], Gennaro Percannella[‡], Mario Vento[‡] and Arnold Wiliem[†]

[*]Sullivan Nicolaides Pathology, Australia
[†]University of Queensland, Australia
[‡]University of Salerno, Italy

Abstract—There has been an ongoing effort in improving reliability and consistency of pathology test results due to their critical role in making an accurate diagnosis. One way to do this is by applying image-based Computer Aided Diagnosis (CAD) systems. This paper proposes a comprehensive benchmarking platform comprising over 1,000 images to evaluate CAD systems for the Anti-Nuclear Antibody (ANA) test via the Indirect Immunofluorescence (IIF) protocol applied on Human Epithelial Type 2 (HEp-2) cells. While prior works in this domain have primarily focussed on classifying individual cell images derived from ANA IIF HEp-2 images, our proposed benchmarking platform goes beyond this by considering the ANA IIF HEp-2 image classification problem. Generally the existing works derive an ANA IIF HEp-2 image label from the dominant pattern of the cell images (we call this approach baseline). In this work, we argue that this approach cannot be used to achieve an acceptable performance, thus, the problem of classifying ANA IIF HEp-2 images (or ANA images in short) is still largely unexplored. To demonstrate that, we propose a simple-yet-effective CAD system which is inspired from the recent success of object bank representation in the object classification domain. We evaluate the proposed system, the baseline and a recent CAD system and show that our proposed system considerably outperforms the others.

I. INTRODUCTION

Pathology tests play a critical role in our healthcare system for patient diagnosis. Any inaccuracies may compromise patient diagnosis and treatment. Applying image-based CAD systems is one of the solutions to leverage test consistency and reliability and also decrease test turn around time [24], [10], [15], [28], [12]. For instance, Tadrous *et al.* proposed a CAD system which can be used for a rapid screening *Ziehl-Neelsen* (ZN)-stained sections for detecting *acid-alcohol-fast bacilli* (AAFB) which cause Tuberculosis (TB) in resource-poor regional areas [24].

The best practice for identifying the existence of connective tissue diseases is via the Anti-Nuclear Antibody (ANA) test using the Indirect Immunofluorescence (IIF) protocol applied on Human Epithelial type 2 (HEp-2) cells [18]. This approach has high sensitivity due to the expression of a wide range of antigens on HEp-2 cells. However, the protocol is [2], [20], [13], [22]: (1) time consuming; (2) labour intensive; (3) subjective; (4) has low reproducibility and (5) has large inter/intra- personnel/laboratory variations. When combined with the subjective analysis by scientists, the results produced from CAD systems can potentially address these issues [10].

In the light of this fact, there has been a surge of interest shown in the literature to develop such systems [10], [19], [13], [5], [14], [22], [4], [29], [23], [1], [25], [26], [11], [16], [3], [21], [6], [31], [9], [8], [32]. This also has been supported by a number of excellent benchmarking platforms such as ICPR2012Contest [10], [9], SNPHEp-2 [31] and ICIP2013 [1] which help the community to compare methods proposed in this area. Existing approaches in image analysis have also been adapted and evaluated [23], [31]. Unfortunately, the existing works primarily focus on the problem of classifying cell images derived from ANA images. Whilst, these work provide significant contribution, the cell classification is only the first step in the whole CAD system procedure. Once the cell patterns have been identified, the system needs to make decision upon the ANA pattern. The identified ANA pattern can then be combined with the scientist opinion. Currently, most approaches classify ANA images by merely using the dominant cell pattern which may only work for a limited number of ANA patterns [10]. Furthermore, these approaches only use the information extracted from the interphase cells.

Each ANA image normally contains a distribution of HEp-2 cells that can be divided into two main cell cycle stages: interphase and mitosis stages (Refer Fig. 1 for some example images of ANA patterns). During the mitosis stage, HEp-2 cells divide into two daughter cells. Unlike the interphase stage, in this stage the amount of cell chromatin is doubled. The cells undergoing the mitosis stage may express different antigens or antigens in different concentration to those of the interphase stage. Therefore, it is essential to use information extracted from both phases to classify an ANA pattern.

In the present work, we argue that the problem of ANA image classification is still largely unexplored. Most existing works primarily use the dominant pattern of the interphase cells in classifying an ANA image (we denote this approach *baseline*). As aforementioned, this is insufficient due to the fact that the information from the mitotic cells is completely ignored. Furthermore, one may have better classification accuracy when the decision is not solely made based on the dominant cell pattern, rather on the information extracted from the cell distribution.

To that end, we first propose a benchmarking platform for ANA image classification allowing the community to evaluate CAD systems designed for ANA image classification. The platform contains a set of ANA images divided into train and test sets along with the standard evaluation protocol. For the immediate benefit to the community, the benchmarking platform is also used in one of the ICPR 2014 contests titled

---

[1]The competition website and dataset available at http://nerone.diiie.unisa.it/contest-icip-2013/index.shtml
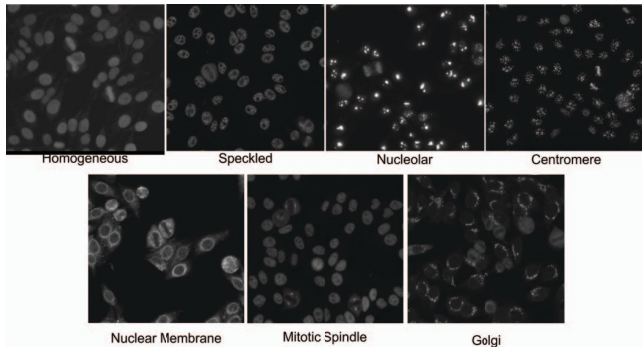
Fig. 1. Some images from the proposed dataset. The first row contains the ANA common patterns whilst the lesser common patterns are presented on the second row.
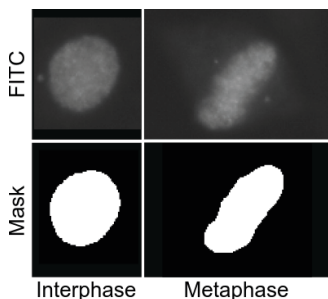

Fig. 2. Example FITC and mask images for interphase and metaphase cells. The mask images are derived from DAPI channel.

the Performance Evaluation of Indirect Immunofluorescence Image Analysis Systems held in conjunction with *the 1st Workshop on Pattern Recognition Techniques for Indirect Immunofluorescence Images* [2].

In this paper, we apply the baseline method and show that it fails to achieve satisfactory results on the proposed benchmarking platform. Then, we propose a simple-yet-effective CAD system, inspired from [17], which uses the information extracted from both mitotic and interphase cells.

We continue our discussion as follows. In the following section, we describe the ANA HEp-2 image classification problem. Section III presents the proposed benchmarking platform. Then we propose our CAD system in Section IV. The comparative evaluation results between the proposed CAD system to the other methods are discussed in Section V. Finally, main findings and future direction are presented in Section VI.

II. THE ANA IIF HEp-2 IMAGE CLASSIFICATION PROBLEM

We use the style of [31] to describe the ANA IIF HEp-2 image classification problem, or ANA image classification problem in short. An ANA image I is represented by the three-tuple $\{I, M, \delta\}$ which consists of: (**i**) the Fluorescein Isothiocyanate (FITC) image channel which carries pattern information I; (**ii**) a binary cell mask image M which are extracted from the *4',6-diamidino-2-phenylindole* (DAPI) image

channel [3]; (**iii**) the fluorescence intensity $\delta = \{\text{weak}, \text{strong}\}$. The goal is to construct a classifier which classifies an image into one of the known ANA classes.

In general, the classifier should have four steps: (1) individual HEp-2 cell image extraction; (2) cell cycle classification; (3) cell image descriptor extraction and classification; (4) ANA image descriptor extraction and classification. The binary mask could be used to extract cell images from the ANA image. We note that that there is a distinct shape between interphase and mitotic cells due to the fact that the DAPI image channel delineates the cell DNA (refer to Fig. 2) Unlike the interphase cells, the cell DNA is centred on the cell undergoing mitosis phase. Despite the fact that one could, in theory, distinguish between mitotic and interphase cells via their shape, we still observed significant errors when only shape information is used (results are not shown). Therefore, we envision that there could be other useful information for addressing the cell cycle classification problem which may improve the classification accuracy (e.g. combining the FITC and the mask images). Once the cells are extracted and their cycle is determined, we can extract their image descriptor and classify them using various approaches proposed from the prior works. In the last step, the system extracts and classifies the ANA image descriptor by using either the classification result of the cells or the cell image descriptor. It is clear from these steps that most prior works largely focus on the third step.

III. THE PROPOSED ANA IMAGE BENCHMARKING PLATFORM

The benchmarking platform consists of a set of ANA images divided into two subsets for training and test. The ANA images were acquired in 2011-2013 from 1,001 ANA positive de-identified patients sera at the Sullivan Nicolaides Pathology Laboratory, Australia. The specimens were prepared with screening dilution 1:80. Then we used a monochrome high dynamic range cooled microscope camera on a microscope with a plan-Apochromat 20x/0.8 objective lens and LED illumination source. We took images from four different locations for each specimen. Specifically, we took one FITC image and one DAPI image for each location. This means, each specimen has eight images (*i.e.* four FITC images with four corresponding mask images). Each image was saved in uncompressed monochrome TIF format with a resolution of 1388 x 1040 pixels [4].

There are seven ANA patterns considered: homogeneous, speckled, nucleolar, centromere, golgi aparatus (Golgi), nuclear membrane (NuMem) and mitotic spindle. As depicted in Fig. 3, the first four patterns are common ANA patterns and the last three are much lesser common or rare. We deliberately combined both common and uncommon patterns to simulate the real scenario where pathology laboratories need to deal with both patterns. We divided the images into two sets: 252 images for training and 749 for testing.

For each individual ANA pattern, we use the standard textual description proposed in [27]:
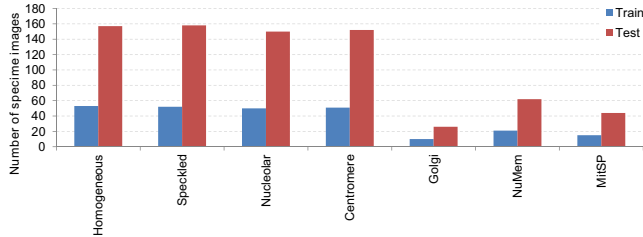

Fig. 3. The number of images per class for each test and training set. There is class imbalance between the common patterns (*i.e.* the first four patterns) and the lesser common patterns (*i.e.* the last three).

- *homogeneous* a uniform diffuse fluorescence covering the entire nucleoplasm sometimes accentuated in the nuclear periphery; In some cases a more intense staining of the inner edge of the nucleus (nuclear rim) can be seen. Some samples may show an additional appearance of peripheral nucleolar staining. Nucleoli are often stained much like the surrounding nucleoplasm. In metaphase and telophase a homogenous or peripheral chromatin staining is seen

- *speckled* the pattern is generally divided into two sub-categories: **coarse speckled**: densely distributed, variable sized speckles, generally associated with larger speckles, throughout the nucleoplasm of interphase cells; nucleoli are negative. Metaphase and telophase cell cytoplasm contains speckles with condensation around the chromatin plate which itself is negative. **fine speckled**: fine speckled staining in a uniform distribution, sometimes very dense so that an almost homogeneous pattern is attained; nucleoli may be positive or negative. Cytoplasm of metaphase cells shows fine speckles and condensation around the chromatin plate which itself is negative. Nuclei of telophase cells may be positive, sometimes being more strongly stained than nuclei of interphase cells

- *nucleolar* brightly clustered large granules corresponding to decoration of the fibrillar centers of the nucleoli as well as the coiled bodies. In mitotic cells the metaphase and telophase plate appear to have a fluorescent irregular "fan-like" edge. Metaphase cell cytoplasm may be slightly positive

- *centromere* rather uniform discrete speckles located throughout the entire nucleus. Telophase and metaphase cells always show these speckles in the condensed chromosomal material

- *golgi aparatus* staining of a polar organelle adjacent to and partially surrounding the nucleus, composed of irregular large granules. Nuclei and nucleoli are negative. Diffuse staining of the cytoplasm of dividing cells sometimes with accentuation around chromosomal material

- *nuclear membrane (NuMem)* a smooth homogeneous ring-like fluorescence of the nuclear membrane in interphase cells; A similar pattern is seen in telophase. In metaphase cells the fluoresence is diffusely localised in the cytoplasm and chromosomal material is unstained

- *mitotic spindle* staining only in the triangular or "banana-shaped" pole area of the mitotic spindle in the metaphase cells

As there is distribution imbalance between the common and lesser common patterns, it is important to define an evaluation protocol which is not biased towards the common patterns. As such we propose to use the mean class accuracy (MCA) to measure a method performance. Technically, we compute the accuracy for each ANA pattern class and then we take the average of the per-class accuracies.

Let CCR_k be the correct classification rate for class k determined as follows.

$$\mathrm{CCR}_k = \frac{1}{N_k}\left(\mathrm{TP_k} + \mathrm{TN_k}\right) \tag{1}$$

where $\mathrm{TP_k}$ and $\mathrm{TN_k}$ are the number of true positive and true negative results on class k, respectively; N_k is the number of ANA images that belong to class k. The mean class accuracy MCA is determined by:

$$\mathrm{MCA} = \frac{1}{K}\sum_{k=1}^{K}\mathrm{CCR}_k \tag{2}$$

where K is the number of pattern classes (*i.e.* K equals seven in this instance).

IV. CELL BANK DESCRIPTOR

In the present work, we derive the ANA image descriptor z_i from the cell bank descriptor extracted from each individual cell image. The cell bank descriptor is inspired from the object bank approach presented in [17]. Technically, each element of the cell bank descriptor is the output score of a one-versus-all SVM classifier specifically trained to detect the existence of a particular cell pattern. Let $\Phi_p : \mathbb{R}^n \mapsto [-1, 1]$ be the p-th one-versus-all SVM classifier which maps an input cell feature descriptor into a continuous value ranging from -1 to 1. Let h_c be the cell bank descriptor of cell c, then the p-th element of h_c is determined by:

$$h_{c,p} = \Phi_p(x_c) \tag{3}$$

where $x_c \in \mathbb{R}^n$ is the image features extracted from the c-th cell image. In other words, $h_c = [\Phi_1(x_c)\ldots\Phi_P(x_c)]$.

We train one SVM classifier for each ANA pattern. In addition, we train a separate set of SVM classifiers for each cell cycle stage. This means, to extract the cell bank descriptor from a cell image, the system needs to determine its cell cycle stage and then apply the corresponding set of SVM classifiers to the cell feature descriptor. Once the cell bank descriptors are extracted from all cells, we compute the average cell bank descriptor for each cell cycle stage:

$$h^{[j]} = \frac{1}{N_j}\sum_{c=1}^{N_i} h_c \tag{4}$$

where j is either interphase or mitosis; N_j is the number cells classified into the j cell cycle stage; h_c is the cell bank

descriptor of the c-th cell which belongs to the j cell cycle stage.

Finally, we represent the i-th ANA image descriptor $z_i \in \mathbb{R}^{2P}$ as the concatenation of the average cell bank descriptor of each cell cycle stage $z_i = [h^{[interphase]} \quad h^{[mitosis]}]$.

Once all the ANA image descriptors have been extracted, we train a multi-class Kernel SVM classifier in conjunction with the Radial Basis Function Kernel. In the present work, we also use Kernel SVM for each one-versus-all SVM classifier in conjunction with Pyramid Match Kernel as suggested in [30].

Unlike the baseline approach that simply assumes the pattern of an ANA image from the most dominant cell pattern, the proposed approach allows more flexibility. More precisely, as the output score for each individual cell classifier is used to represent each cell image, the proposed approach assumes that each cell could belong to one or more patterns (*e.g.* when a cell is classified as positive by two cell classifiers). This means, to some extend, the cell bank descriptor captures the information about the distribution of cell patterns appeared within the ANA image.

V. EVALUATION

We first present the experiment settings and then we contrast the proposed CAD system, here denoted *Cell Bank*, to the baseline method and the Multiple Expert System (MES) [22].

A. Experiment settings

Each cell image is represented by using the Cell Pyramid Matching (CPM) descriptor due to its robustness in various laboratory settings [30]. However, our method is not limited to this descriptor. The CPM descriptor consists of three histograms: (1) the overall cell histogram; (2) the histogram extracted from the cell interior; (3) the histogram extracted from the cell boundary. Each histogram is extracted by using the Soft Assignment encoding method with Discrete Cosines Transform (DCT) patch level descriptor. We use 1024 dictionary atoms for each histogram.

We use a multi-class Kernel SVM classifier to classify individual cell images for the baseline method. It then derives a given ANA image label from the dominant cell pattern. We also implemented the Multiple Expert System, here denoted MES, proposed in [22]. In MES, each cell pattern has a binary KSVM classifier in conjunction with the Radial Basis Function Kernel. To classify an ANA image, MES will compute the weighted voting score wherein the weight is determined from the classifier reliability score.

B. Evaluation on various settings

In this evaluation we varied the settings of the proposed approach. We compared the efficacy between Kernel SVM and Nearest Neighbour classifiers as the ANA image classifier. We also evaluated the usefulness of the information provided from each cell cycle stage and when both were combined.

The results shown in Table I suggest that the interphase cells carry more useful information than mitotic cells. Nevertheless, combining the information from both gives the best

TABLE I. PERFORMANCE COMPARISON OF THE PROPOSED APPROACH VARIANTS. NN: NEAREST NEIGHBOUR; KSVM: KERNEL SUPPORT VECTOR MACHINE.

Variants	Mean class accuracy (in %)
Interphase - NN	70.9
Mitotic - NN	53.0
Both - NN	73.3
Interphase - KSVM	72.0
Mitotic - KSVM	56.3
Both - KSVM	**79.3**

TABLE II. PERFORMANCE COMPARISON OF THE MES APPLIED ON THE INTERPHASE AND MITOTIC CELLS.

Variants	Mean class accuracy (in %)
Interphase - MES	**66.4**
Mitotic - MES	53.0

performance. In addition, we also found that KSVM is a better classifier than the Nearest Neighbour.

Table II presents the evaluation of the MES approach on both cells. The MES proposed in [22] only considers interphase cells, however, in this work, we also present the results on mitotic cells as well. The results are still consistent with the previous findings in Table I suggesting that interphase cells carry more information.

It is noteworthy to mention that the results presented here are much lower and seem to contradict the results reported in [22]. On closer examination we found that some classifiers have large classification errors due to confusion in ANA patterns that do not have dominant cell patterns. For instance, the mitotic spindle pattern does not have a specific interphase cell pattern. In fact the pattern could be similar to either homogeneous or speckled. This decreases the reliability score which in turns could force the system to choose the incorrect ANA pattern class which has a better reliability score.

C. Comparative evaluation of systems

In this section we compare the best performing system found from the previous section to the baseline. Fig. 4 presents the evaluation results. The proposed approach outperforms both MES and the baseline. There is a slight improvement on the proposed approach when using interphase cells compared to the baseline.

Table III shows further detail of the per-class accuracy results. The proposed approach performs much better in all classes except with Nucleolar. We found that the proposed approach significantly improves the performance of less common patterns such as Golgi and Mitotic Spindle. However, when only interphase cells are used, it has worse performance in common patterns compared to the baseline. The mitotic cells play an important role in improving the performance on almost all patterns. The highest improvement was achieved with the Speckled pattern.

Another noteworthy observation is that, although the mitotic spindle pattern is only found in the mitotic cells, its performance has not changed even when the proposed approach uses the mitotic cell information. This finding warrants further investigation.
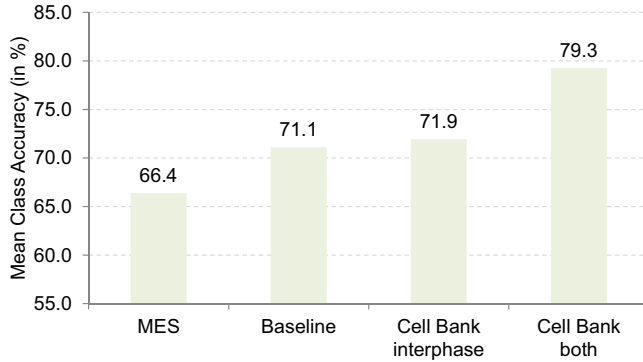
Fig. 4. Comparative evaluation between the proposed Cell Bank approach, the Multiple Expert System (MES) [22] and the baseline; The proposed cell Bank both uses information from both interphase and mitotic cells.

TABLE III. PER-CLASS ACCURACY FOR THE BASELINE, MES, AND THE PROPOSED CELL BANK (CB) SYSTEM. HO: HOMOGENEOUS; SP: SPECKLED; NUC: NUCLEOLAR; CE: CENTROMERE; GO: GOLGI APARATUS; NU: NUCLEAR MEMBRANE; MI: MITOTIC SPINDLE.

CAD system	Per-Class Accuracy (in %)						
	Ho	Sp	Nuc	Ce	Go	Nu	Mi
MES - interphase [22]	58.0	56.3	95.3	95.4	65.4	**80.6**	13.6
Baseline	88.5	69.6	**96.7**	94.7	57.7	67.7	22.7
CB - interphase - KSVM	74.5	74.7	92.7	92.1	65.4	58.1	38.6
CB - both - KSVM	**89.8**	**88.6**	95.3	**98.0**	65.4	79.0	**38.6**

VI. CONCLUSIONS

There has been a great effort to develop CAD systems for the ANA test via the Indirect Immunofluorescence protocol applied on HEp-2 cells. When combined with the manual results from scientists, the CAD system results could potentially leverage test consistency and reliability as well as decrease the test turn around time. Despite much interest, prior works in this domain have primarily focussed on classifying individual cell images derived from ANA IIF HEp-2 images. In the present work, we take a further step by considering the problem of ANA IIF HEp-2 image classification. Our major contribution is on the proposed benchmarking platform which could stimulate further exploration in this field. The benchmarking platform consists of a set of specimen images acquired from 1,001 patient sera as well as the evaluation metric for comparative analysis. In addition, we have shown that using the dominant cell pattern to determine the pattern of a given ANA IIF HEp-2 image, the approach used by most prior works, is insufficient to achieve satisfactory performance. To prove this argument, we proposed a simple-yet-effective CAD system, namely Cell Bank, which was inspired from the object bank approach. When compared to the baseline as well as a recent CAD system on the proposed benchmarking platform, the proposed Cell Bank significantly outperformed the other methods.

We note that although the proposed mean class accuracy (MCA) metric gives us good performance measurement, there are other approaches that we would like to explore in the future such as Average Precision (AP) and Precision-Recall curve used in the PASCAL object categorisation challenges [7].

REFERENCES

[1] W. Bel Haj Ali, P. Piro, D. Giampaglia, T. Pourcher, and M. Barlaud. Biological cell classification using bio-inspired descriptor in a boosting k-NN framework. In *International Conference on Pattern Recognition (ICPR)*, 2012.

[2] N. Bizzaro, R. Tozzoli, E. Tonutti, A. Piazza, F. Manoni, A. Ghirardello, D. Bassetti, D. Villalta, M. Pradella, and P. Rizzotti. Variability between methods to determine ANA, anti-dsDNA and anti-ENA autoantibodies: a collaborative study with the biomedical industry. *Journal of Immunological Methods*, 219(1-2):99–107, 1998.

[3] S. D. Cataldo, A. Bottino, E. Ficarra, and E. Macii. Applying textural features to the classification of hep-2 cell patterns in iif images. In *International Conference on Pattern Recognition (ICPR)*, 2012.

[4] E. Cordelli and P. Soda. Color to grayscale staining pattern representation in IIF. In *International Symposium on Computer-Based Medical Systems*, pages 1–6, 2011.

[5] P. Elbischger, S. Geerts, K. Sander, G. Ziervogel-Lukas, and P. Sinah. Algorithmic framework for HEp-2 fluorescence pattern classification to aid auto-immune diseases diagnosis. In *IEEE International Symposium on Biomedical Imaging: From Nano to Macro*, pages 562–565, 2009.

[6] I. Ersoy, F. Bunyak, J. Peng, and K. Palaniappan. HEp-2 cell classification in IIF images using shareboost. In *International Conference on Pattern Recognition (ICPR)*, 2012.

[7] M. Everingham, L. Van Gool, C. K. I. Williams, J. Winn, and A. Zisserman. The pascal visual object classes (voc) challenge. *International Journal of Computer Vision*, 88(2):303–338, jun 2010.

[8] M. Faraki, M. T. Harandi, A. Wiliem, and B. C. Lovell. Fisher tensors for classifying human epithelial cells. *Pattern Recognition*, 47(7):2348–2359, 2014.

[9] P. Foggia, G. Percannella, A. Saggese, and M. Vento. Pattern recognition in stained hep-2 cells: Where are we now? *Pattern Recognition*, 47:2305–2314, 2014.

[10] P. Foggia, G. Percannella, P. Soda, and M. Vento. Benchmarking hep-2 cells classification methods. *IEEE transactions on medical imaging*, 2013.

[11] S. Ghosh and V. Chaudhary. Feature analysis for automatic classification of hep-2 florescence patterns: Computer-aided diagnosis of autoimmune diseases. In *International Conference on Pattern Recognition (ICPR)*, 2012.

[12] M. N. Gurcan, L. E. Boucheron, A. Can, A. Madabhushi, N. M. Rajpoot, and B. Yener. Histopathological image analysis: A review. *Biomedical Engineering, IEEE Reviews in*, 2:147–171, 2009.

[13] R. Hiemann, T. Bttner, T. Krieger, D. Roggenbuck, U. Sack, and K. Conrad. Challenges of automated screening and differentiation of non-organ specific autoantibodies on HEp-2 cells. *Autoimmunity Reviews*, 9(1):17–22, 2009.

[14] T. Hsieh, Y. Huang, C. Chung, and Y. Huang. HEp-2 cell classification in indirect immunofluorescence images. In *Int. Conf. Information, Communications and Signal Processing*, pages 1–4, 2009.

[15] R. D. Labati, V. Piuri, and F. Scotti. All-IDB: the acute lymphoblastic leukemia image database for image processing. In *2011 18th IEEE International Conference on Image Processing (ICIP)*, pages 2045–2048. IEEE, Sept. 2011.

[16] K. Li and J. Yin. Multiclass boosting svm using different texture features in hep-2 cell staining pattern classification. In *International Conference on Pattern Recognition (ICPR)*, 2012.

[17] L.-J. Li, H. Su, E. P. Xing, and L. Fei-Fei. Object bank: A high-level image representation for scene classification & semantic feature sparsification. In *the Neural Information Processing Systems (NIPS)*, 2010.

[18] P. L. Meroni and P. H. Schur. ANA screening: an old test with new recommendations. *Annals of the Rheumatic Diseases*, 69(8):1420 – 1422, 2010.

[19] P. Perner, H. Perner, and B. Mller. Mining knowledge for HEp-2 cell image classification. *Artificial Intelligence in Medicine*, 26:161–173, 2002.

[20] B. Pham, S. Albarede, A. Guyard, E. Burg, and P. Maisonneuve. Impact of external quality assessment on antinuclear antibody detection performance. *Lupus*, 14(2):113–119, 2005.

[21] V. Snell, W. Christmas, and J. Kittler. Texture and shape in fluorescence pattern identification for auto-immune disease diagnosis. In *International Conference on Pattern Recognition (ICPR)*, 2012.

[22] P. Soda and G. Iannello. Aggregation of classifiers for staining pattern recognition in antinuclear autoantibodies analysis. *IEEE Trans. Information Technology in Biomedicine*, 13(3):322–329, 2009.

[23] P. Strandmark, J. Ulén, and F. Kahl. Hep-2 staining pattern classification. In *Int. Conf. Pattern Recognition*, 2012.

[24] P. J. Tadrous. Computer-assisted screening of ziehl-neelsen-stained tissue for mycobacteria. algorithm design and preliminary studies on 2,000 images. *American Journal of Clinical Pathology*, 133(6):849–858, June 2010.

[25] I. Theodorakopoulos, D. Kastaniotis, G. Economou, and S. Fotopoulos. Hep-2 cells classification via fusion of morphological and textural features. In *IEEE International Conference on Bioinformatics and Bioengineering (BIBE)*, 2012.

[26] G. Thibault and J. Angulo. Efficient statistical/morphological cell texture characterization and classification. In *International Conference on Pattern Recognition (ICPR)*, 2012.

[27] A. S. Wiik, M. Hier-Madsen, J. Forslid, P. Charles, and J. Meyrowitsch. Antinuclear antibodies: A contemporary nomenclature using HEp-2 cells. *Journal of Autoimmunity*, 35:276 – 290, 2010.

[28] D. C. Wilbur. Digital cytology: current state of the art and prospects for the future. *Acta Cytologica*, 55(3):227–238, 2011.

[29] A. Wiliem, P. Hobson, R. Minchin, and B. Lovell. An automatic image based single dilution method for end point titre quantitation of antinuclear antibodies tests using HEp-2 cells. In *Digital Image Computing: Techniques and Applications*, Noosa, Australia, 2011.

[30] A. Wiliem, C. Sanderson, Y. Wong, P. Hobson, R. F. Minchin, and B. C. Lovell. Automatic classification of human epithelial type 2 cell indirect immunofluorescence images using cell pyramid matching. *Pattern Recognition*, 47(7):2315 – 2324, 2014.

[31] A. Wiliem, Y. Wong, C. Sanderson, P. Hobson, S. Chen, and B. C. Lovell. Classification of human epithelial type 2 cell indirect immunofluoresence images via codebook based descriptors. In *IEEE Workshop on Applications of Computer Vision (WACV)*, 2013.

[32] Y. Yang, A. Wiliem, A. Alavi, B. C. Lovell, and P. Hobson. Visual learning and classification of human epithelial type 2 cell images through spontaneous activity patterns. *Pattern Recognition*, 47(7):2325–2337, 2014.